Liao, Y., Cheng, Z., Zuo, W., Thomas, A., & Faul, C. FJ. (2017). Nitrogen-rich conjugated microporous polymers: facile synthesis, efficient gas storage and heterogeneous catalysis. *ACS Applied Materials and Interfaces*, *9*(44), 38390-38400. https://doi.org/10.1021/acsami.7b09553

Nitrogen-Rich Conjugated Microporous Polymers: Facile Synthesis, Efficient Gas storage and Heterogeneous Catalysis

Yaozu Liao,[,1,2,3] Zhonghua Cheng,[1] Weiwei Zuo,[1] Arne Thomas[*,2] Charl F. J. Faul[*,3]*

[1]State Key Laboratory for Modification of Chemical Fibers and Polymer Materials & College of Materials Science and Engineering, Donghua University, Shanghai 201620, China
[2]Department of Chemistry and Functional Materials, Technische Universität Berlin, Berlin 10623, Germany
[3]School of Chemistry, University of Bristol, Bristol, England BS8 1TS, UK

**Corresponding authors: yzliao@dhu.edu.cn; arne.thomas@tu-berlin.de; charl.faul@bristol.ac.uk*

Abstract: Nitrogen-rich conjugated microporous polymers (NCMPs) have attracted great attention in recent years owing to their polarity, basicity, and ability to coordinate metal ions. Herein three NCMPs, structurally close to polyaniline, were facilely synthesized via chemical oxidative polymerization between multi-connected aniline precursors. The NCMPs with high N content (11.84 wt%), intrinsic ultramicroporosity (<1 nm) and moderate surface area (485 $m^2 g^{-1}$), show wide-ranging adsorption functionality, e.g. CO_2 uptake (11 wt%) and CO_2-selectivity over N_2 (360, 1 bar), 1.0 wt% H_2 storage as well as 215 wt% iodine vapor uptake at ambient pressure. Moreover, these NCMPs act as support for palladium catalysts and can maintain >94% activity in Suzuki–Miyaura coupling reactions after six continuous runs.

Keywords: Conjugated microporous polymers, polyaniline, gas storage, catalysis, synthesis

Introduction

Conjugated microporous polymers (CMPs) with small pores (<2 nm), large surface areas, high chemical stability, low density and reversible redox properties, are of great interest for a variety of applications.[1-3] These porous materials have been widely investigated since discovery in 2007, both for fundamental reasons and because of their potentials for application in areas of gas adsorption,[4] heterogeneous catalysis,[5] and electrochemical energy storage.[6] Over the past decade, various aromatic functional building blocks have been incorporated into CMPs for extended applications such as sensors,[7,8] light harvesting,[9] organic light-emitting diodes,[10,11] and

photocatalysis.[12-14]

The porosity of CMPs is largely determined by their backbone structure, although solvent-templating effects can also contribute.[15,16] Generally, CMPs are synthesized via well-developed transition-metal-catalyzed coupling reactions such as the Suzuki,[9] Yamamoto,[17] Sonogashira,[18,19] and Buchwald-Hartwig reactions.[20,21] Expensive (noble) metal-based catalysts or mediators are however needed for their synthesis. Recently, chemical oxidative polymerizations of carbazole,[22-24] thiophene,[25-27] and pyrrole-based precursors[28,29] have been utilized to generate CMPs, using commonly available iron (III) chloride as the oxidant. Electrochemical polymerization of these precursors has also been used to yield CMP thin films on electrodes.[10,11,26] While oxidative polymerization for CMP generation has mainly focused on carbazole and thiophene-based polymers, to the best of our knowledge, the synthesis of highly cross-linked 3D polyaniline networks with intrinsic microporosity and high N content has rarely been reported, and only performed through the addition of cross-linkers.[30]

Polyaniline, a prototypical nitrogen-rich conjugated polymer, has emerged as a very important semiconductor that is particularly attractive for electronics and energy storage devices.[31-33] Microporosity introduced to such organic semiconductors may provide desired interface properties, such as interpenetration with a second material, enabling better gas or charge separation, and sensing properties via interactions with the electron pool.[34-36] For example, the incorporation of polyaniline into the porous metal-organic framework MIL-101 could dramatically increase the CO_2-selective uptake ability owing to the functionality of the nitrogen centers.[36]

Nitrogen-rich conjugated microporous polymers (NCMPs) could furthermore be of interest owing to their polarity, basicity, and ability to coordinate metal ions. Herein we report three NCMPs structurally close to conventional polyaniline, which are synthesized via simple chemical oxidative polymerization of multi-connected aniline precursors. Using this simple technique, we are, for the first time, able to prepare polyaniline-like microporous materials with high nitrogen contents. As-prepared porous materials benefit from the high nitrogen density to obtain materials with good CO_2/N_2 selectivities, and moderate CO_2, H_2, and iodine uptake capacities at ambient pressure. The materials also act as excellent supports for Suzuki-Miyaura reaction catalysts, showing high stability and recyclability. Beyond these areas, such NCMPs might furthermore

open new avenues and enable new possibilities for advanced optoelectronic applications.

Results and discussion

Three multi-connected aniline precursors (**P1**, **P2**, and **P3**) were synthesized via Buchwald-Hartwig coupling between aniline and the tribromoaryl monomers **M1**, **M2**, and **M3**, respectively (Scheme 1, see a detailed characterization of monomers and polymers, and related discussions in supporting information). Chemical oxidative polymerization of these precursors in chloroform ($CHCl_3$) was carried out using stoichiometric amounts of $FeCl_3$ dissolved in nitromethane (CH_3NO_2) as the reaction medium. The reactions started immediately, as seen from the rapid formation of black precipitates. After filtration and extensive purification using $CHCl_3$, concentrated HCl (35 wt%), and hot water (75 ºC), **NCMP1**, **NCMP2**, **NCMP3** products were obtained as brown to dark grey powders (Figure 1a) in nearly quantitative yields, indicating a high degree of polymerization.

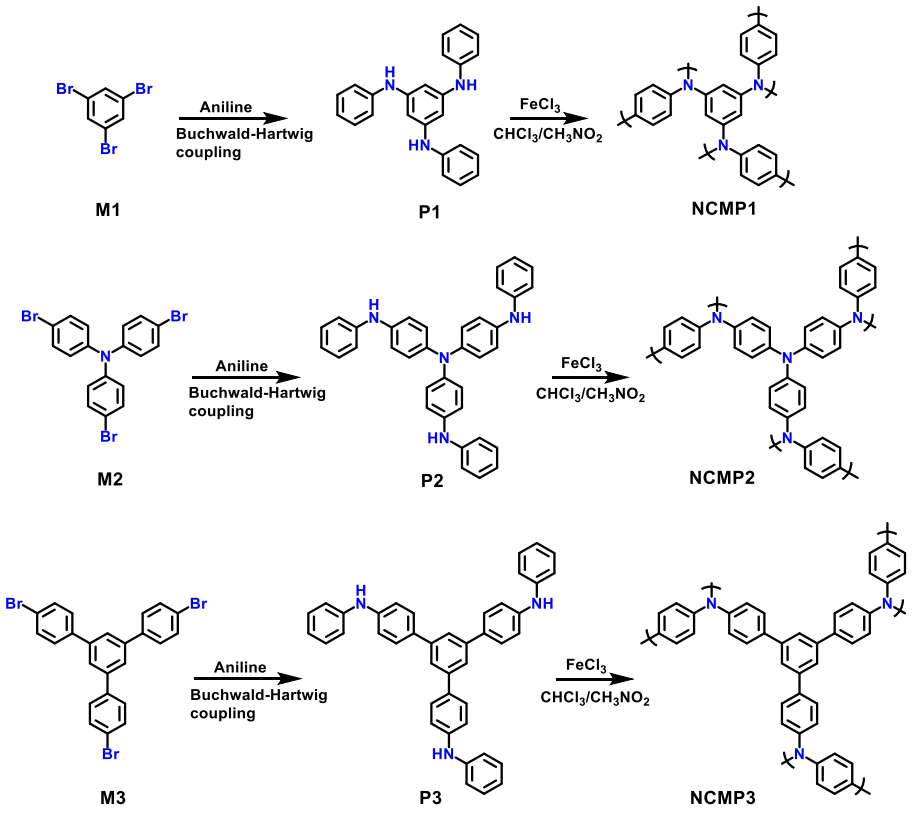

Scheme 1 Synthetic route to nitrogen-rich CMP networks (**NCMP1**, **NCMP2**, **NCMP3**).

It is well known that oxidative polymerization of aniline and its *N*-substituted derivatives such as *N*-methylaniline occurs generally *via* head-to-tail coupling of the most negatively-charged N

atoms and unsubstituted C_4 atoms.[37] On the basis of atomic electron populations and spin-density simulations of precursors at a B3LYP/6-31G (*d*) level using Gaussian 09 software[38] (Figs. S1-6 and Tables S1-6, see detailed discussions in supporting information), chemical oxidative polymerization of **P1**, **P2**, and **P3** most probably yielded polymer networks **NCMP1**, **NCMP2** and **NCMP3**, respectively, as shown in Scheme 1 and Figure S7. The Fourier transform infrared (FT-IR) spectra of NCMPs showed that the peaks at ~3380 cm^{-1} owing to the stretching vibration of the secondary amine (PhNHPh) became much less intensive, indicating that most of these groups are converted into tertiary amines (Ph_3N) (Figure S8). Three distinct peaks at 1598, 1498, and 820 cm^{-1} originated from the precursors owing to C–N, C=C, and aryl C–H bands,[31-33] respectively, present in all the NCMPs, further suggesting a successful coupling. Further characterization of the chemical composition of the formed NCMPs was confirmed by inductively coupled plasma-atomic emission spectrometry (ICP-AES), energy dispersive X-ray spectroscopy (EDX), solid-state ^{13}C cross-polarization magic angle spinning nuclear magnetic resonance (^{13}C CP/MAS NMR), and ultraviolet-visible/near infrared (UV-Vis/NIR) spectroscopies. ICP-AES and EDX measurements confirmed negligible Fe (0.05-0.07 wt%) and high N contents (7.39-11.84 wt%) in the products after extensive purification. Solid-state ^{13}C CP/MAS NMR spectra of polymers show two main resonances at ~141 and ~128 ppm, originating from N- and H-substituted benzene rings,[20,21] respectively (Figure 1b). Note that the spectrum of **NCMP3** shows an additional resonance at ~113 ppm, due to the C-substituted benzene rings. Solid-state UV–Vis/NIR spectra of the polymers show a narrow peak at ~320 nm and a broad peak in the range 700-1300 nm (Figure 1c). The observed absorption spectra of **NCMP1** and **NCMP2** are comparable to that of traditional polyaniline, owing to the close resemblance to the molecular structure of polyaniline.[31-33] Compared to **NCMP3**, **NCMP1** and **NCMP2** show much more intensive broad peaks in the 700-1300 nm range, indicating a higher doping level. The Cl atom content of as-synthesized polymers was tested to understand the doping level of the materials. As determined by EDX measurements, **NCMP1**, **NCMP2**, and **NCMP3** still contain 5.6, 4.2, and 1.2 wt% of Cl, respectively. It can be reasoned that the higher Cl content found in **NCMP1** and **NCMP2** are due to the more basic triphenylamine units present. The byproduct of HCl resulted from the chemical oxidative polymerization more readily doped with **NCMP1** and **NCMP2** rather

than **NCMP3**.

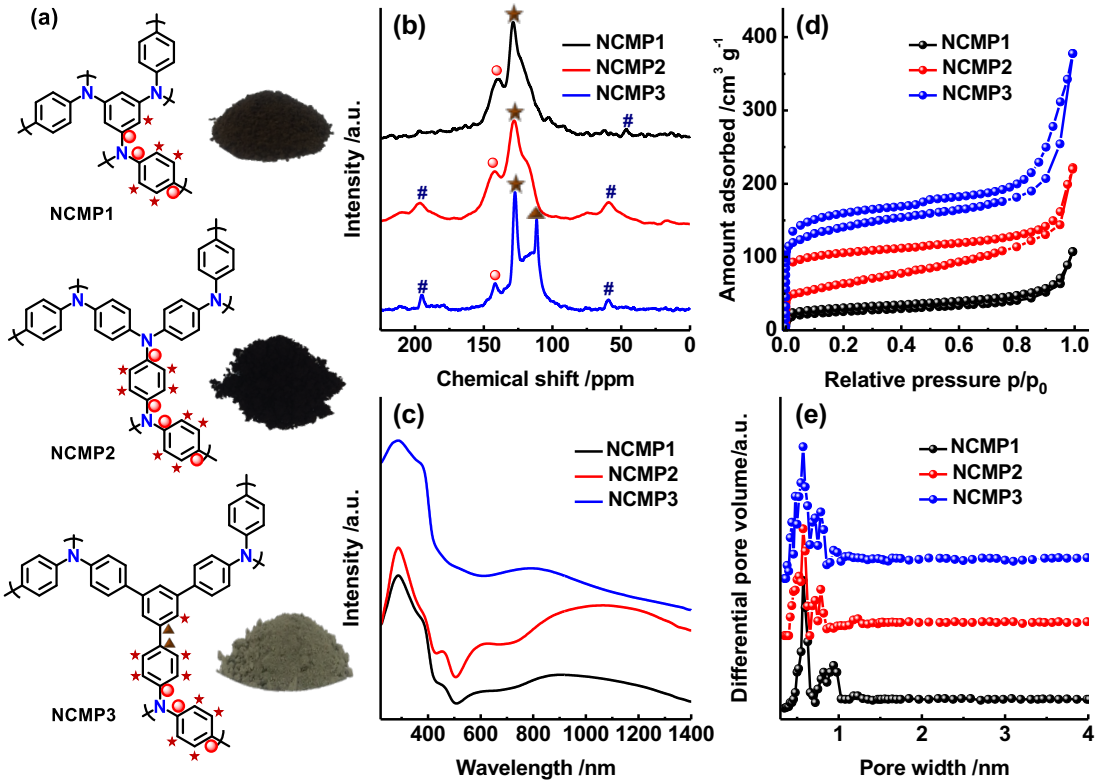

Figure 1 (a) Chemical structures/photographs, (b) solid-state ^{13}C CP/MAS NMR spectra, (c) UV-Vis/NIR spectra, (d) N_2 adsorption/desorption isotherms, and (e) pore widths of NCMPs. The symbol # in Figure 1b represents spinning side band.

Scanning electron microscope (SEM) and transmission electron microscope (TEM) images show that the NCMPs consist of aggregated nanoparticles (Figure 2) resulting in some large meso and macropores due to the presence of interstitial voids. High-resolution TEM images also indicate microporous structures. As indicated by thermogravimetric analyses (TGA) carried out in nitrogen (Figure S9), the weight-loss of three polymers at the beginning (0-200 ºC) of the analysis follows the order: **NCMP1** > **NCMP2** > **NCMP3**, which is well consistent with the amount of residual HCl. When heated to 900 ºC, the highly cross-linked NCMPs maintained 55-69 wt% carbonaceous residues, which is in contrast to conventional polyaniline yielding no carbonaceous residue.

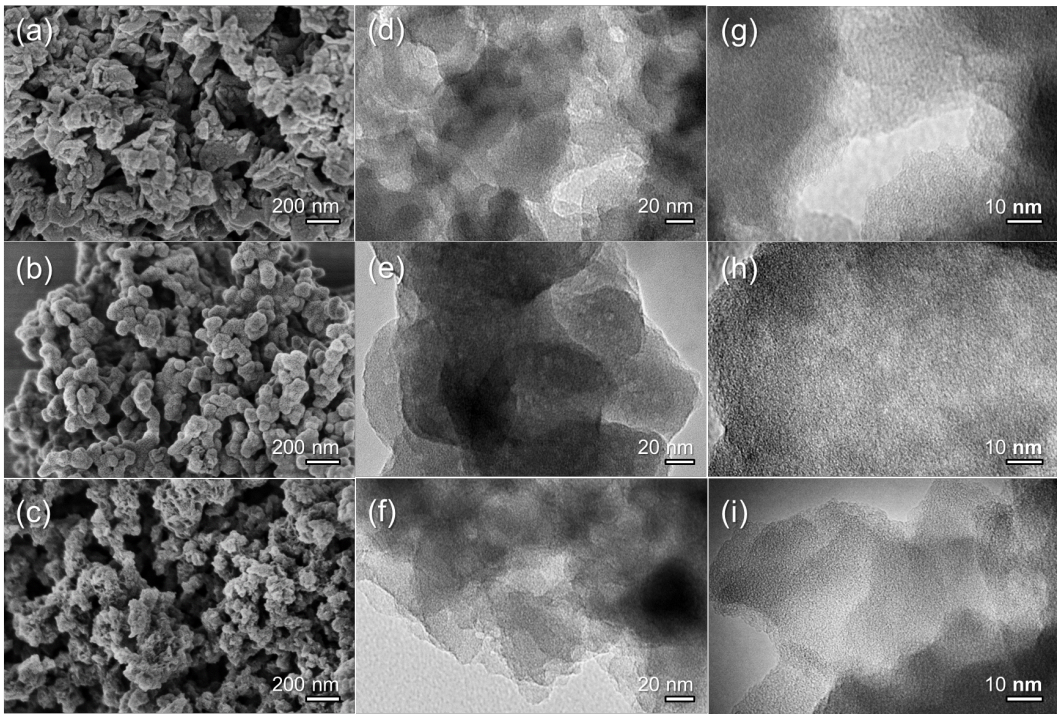

Figure 2 (a-c) SEM and (d-i) TEM images of (a,d,g) **NCMP1**, (b,e,h) **NCMP2** and (c,f,i) **NCMP3** networks at low (d-f) and high (g-i) magnifications.

Microporosity of the NCMPs was confirmed by N_2 adsorption measurements. **NCMP1**, **NCMP2**, and **NCMP3** (Figure 1d) reveal Brunauer–Emmett–Teller (BET) surface areas of 58, 280, and 485 $m^2\ g^{-1}$, total pore volumes of 0.15, 0.30, and 0.57 $cm^3\ g^{-1}$ at a relative pressure of $p/p_0 = 0.994$, and micropore volumes of 0.06, 0.09, and 0.13 $cm^3\ g^{-1}$, respectively (Table 1). On the basis of the N_2 adsorption isotherms, the NCMPs possess small micropores with sizes below 1 nm as determined by the nonlocal density functional theory (NLDFT) method (Figure 1e).

As discussed above, the NCMP networks mainly consist of the triphenylamine (NPh_3) moiety, known as a hole-transporting material for organic electroluminescent devices,[39] as well as an important tecton yielding high surface area CMPs.[21,40,41] Applying our NCMPs for gas storage and as catalytic support is therefore worthy of exploration. All NMCPs exhibit CO_2 storage capability (Figure 3a,b and Table 1), with **NCMP3** showing the highest CO_2 uptake capacity (11 wt%, 2.50 mmol g^{-1}) at 1 bar and 273 K. The CO_2 uptake capacity obtained is comparable or even superior to that of many porous materials including polyaniline@MIL-101 (<2.26 mmol g^{-1}),[36] covalent organic frameworks (COF-1, 5, 8, 10, 102, 103 and TpBa, 1.38-2.37 mmol g^{-1}),[42] and CMPs (CMP-0, 5, TCMP-5, TFM-1, CMP-1-NH_2, CMP-1-COOH, 1.1-2.1 mmol g^{-1}),[43-45] although it is

lower than that of the optimal CTFs i.e. CTF-0 (4.22 mmol g^{-1})[46] and CTF-P6M (4.17 mmol g^{-1})[47] with a much higher N content. Besides the CO_2 uptake capacity, high CO_2 selectivity over N_2 is also a critical factor for real carbon capture applications. Therefore, we measured the N_2 adsorption of the NCMPs at 273 K to examine their potential ability to separate gases. On the basis of ideal adsorbed solution theory (IAST) calculations (Figure S10, Tables S7,8, see details in supporting information), we found that CO_2-selectivities over N_2 are controlled by the molecular architecture (Figure 3c,d). Two compositions of CO_2/N_2 gas mixtures (15/85 and 25/75) were applied for calculation. The results show that the selectivity largely depends on the type of NCMP: **NCMP1**, synthesized from smallest precursor **P1** with the highest nitrogen content (11.84 wt%), shows the highest selectivities with values up to 188 and 360 at 1 bar for the two tested gas mixtures, respectively. The selectivity obtained from **NCMP1** is higher than that of recently reported porous materials such as porous organic polymers (40-78),[48] nitrogen-rich carbons (11-76),[49] and MOFs (93)[50].

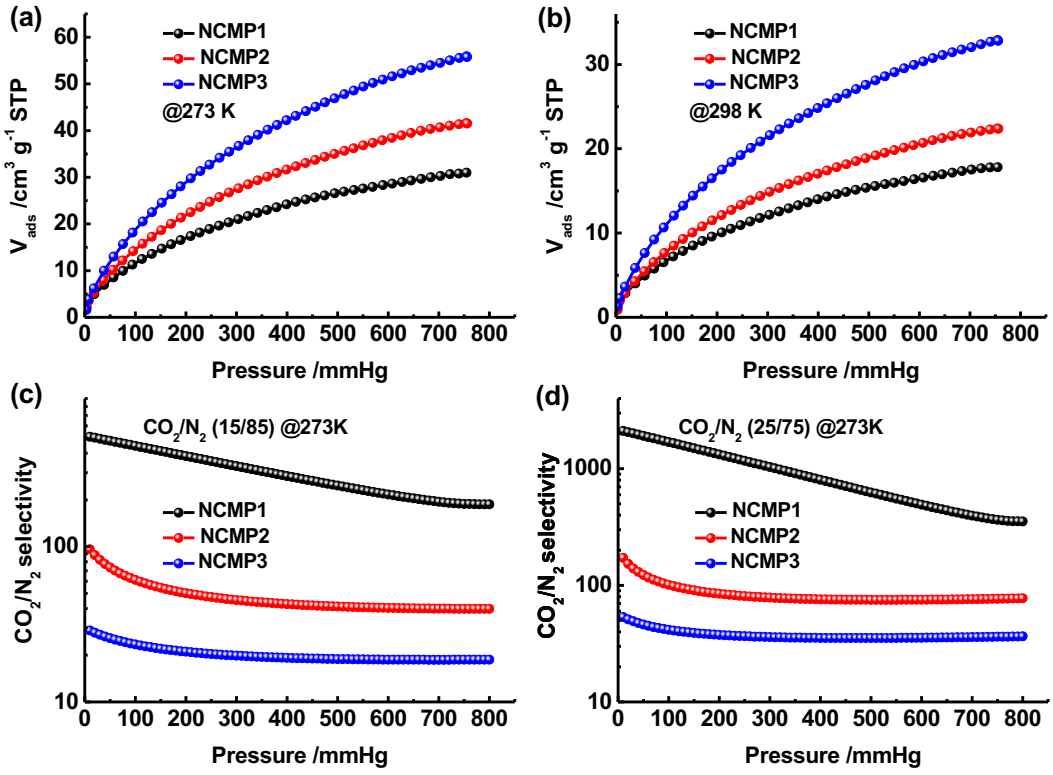

Figure 3 (a,b) CO_2 adsorption isotherms of NCMPs at 273 and 298 K; (c,d) CO_2-selectivities of NCMPs over N_2 using 15/85 and 25/75 compositions of CO_2/N_2 gas phases for calculations.

To explore the interaction between CO_2 and the pore surfaces of the NCMP networks, the isosteric heat of adsorption (Q_{st}) was calculated based on the Clausius-Clapeyron equation using single gas adsorption isotherms[51] (Figure S11). Initial Q_{st} values for CO_2 adsorption were found as high as 33.6, 31.6, and 31.0 kJ mol^{-1} for **NCMP1**, **NCMP2**, and **NCMP3**, respectively, which are higher than those values reported for many other porous organic/inorganic adsorbents such as microporous polymer networks (15.6-29.8 kJ mol^{-1}),[52] MOFs (15-30 kJ mol^{-1}),[53] and carbons (20 kJ mol^{-1})[54]. However, the values remain below the typical energy of chemisorption (Q_{st} >40 kJ mol^{-1}),[55] implying strong physical interactions between adsorbed CO_2 and the functional pore surface. Moreover, the NCMPs show H_2 storage capacities up to 1.02 wt% at 77 K and 1.0 bar (for example, **NCMP3**) (Figure S12), which is higher than the values obtained for most porous polymer networks,[56,57] for example, a recent report on porous hypercrosslinked polymers showed H_2 storage capacities of 1.01 wt% (77 K and 1.13 bar).[57] Again, on the basis of the Clausius-Clapeyron equation,[58] initial Q_{st} values for H_2 adsorption in **NCMP1** is calculated as high as 8.3 kJ mol^{-1} (Figure S13). This value is higher than that of other porous organic polymers such as of PAF-1 (4.6 kJ mol^{-1}),[59] PIs (5.3-7.0 kJ mol^{-1}),[60] COFs (6.0-7.0 kJ mol^{-1}),[61-63] further suggesting a favorable physical interaction between adsorbed H_2 and the porous surface.[64]

Table 1 Summaries of physiochemical properties of NCMPs.

Polymer	S_{BET}[a]	V_T[b]	V_{micro}[c]	N%[d]	CO_2 uptake at 1 bar (wt%)		H_2 uptake at 1 bar (wt%)	
	(m^2/g)	(cm^3/g)	(cm^3/g)	(wt%)	273 K	298 K	77 K	87 K
NCMP1	58	0.15	0.06	11.84	6.1	3.5	0.68	0.49
NCMP2	280	0.30	0.09	10.14	8.2	4.4	0.79	0.54
NCMP3	485	0.57	0.13	7.39	11.0	6.5	1.02	0.68

[a]calculated using a multi-point BET method; [b]calculated based on N_2 adsorption at p/p_0 = 0.994; [c]calculated using a MP method; [d]relative content measured by EDX.

In addition to CO_2 and H_2 storage, we also explored the NCMP networks for their potential application in iodine adsorption. Iodine vapor adsorption is of particular interest, since the long-lived radioactive iodine isotopes (e.g. ^{129}I or ^{131}I) need to be removed from exhaust fumes of

nuclear power plants regularly.[65] Previous studies showed that nitrogen-containing CMPs are promising to address this issue.[20] Upon exposure to iodine vapor at 1 bar and 358 K, porous NCMPs became gradually darker as iodine molecules diffused into the porous networks. Equilibrium adsorption is found to be 215, 186, and 161 wt% for **NCMP1**, **NCMP2**, and **NCMP3**, respectively. It is well known that electron-deficient iodine (acceptor) interacts with electron-rich adsorbents (donor), giving rise to charge transfer from the HOMO of the donor to the LUMO of the acceptor. Previous studies suggest that the charge-transfer interactions are responsible for the high iodine adsorption capacity of aniline-linked hexaphenylbenzene-based conjugated microporous polymer (HCMP) adsorbents.[20] The NCMPs showed a slightly smaller main pore size than the molecular diameter of iodine (0.57 vs. 0.60 nm), as determined by the nitrogen adsorption isotherms at 77 K. We believe that the combination of nitrogen content and HOMO energy of the NCMPs (both which influence the electron-donor ability) may preferentially direct the iodine adsorption capacity rather than surface area and pore size (determined by nitrogen adsorption at 77 K).[66] We used **P1**, **P2**, and **P3** as model compounds to monitor the HOMO energy of corresponding polymers on the basis of calculations at the B3LYP/6-31G (*d*) level with Gaussian 09 software.[38] **NCMP1**, with the highest nitrogen content, shows the highest HOMO energy (Table S9), which fits very well with the highest iodine adsorption capacity observed. Actual measurements of HOMO-LUMO band gaps for polymers were carried out using cyclic voltammetry (Figure S14) and UV-vis absorption scans (Figure 1c). The HOMO-LUMO band gaps (E_g) of **NCMP1**, **NCMP2**, and **NCMP3** were calculated on the basis of the wavelengths at maximal UV-vis absorption (λ_{max}) according to the equation: $E_g = 1240/\lambda_{max}$, giving values for E_g = 1.22, 1.17, and 1.54 eV, respectively. The results indicate that the electron-donating ability follows the order: **NMCP2** > **NCMP1** >> **NCMP3**, which is also seen in the strongest redox activity of **NCMP2** according to cyclic voltammetry measurements (Figure S14).

Previous studies showed that reduction and oxidization of secondary amine-linked HCMPs resulted in better iodine and CO_2 uptake capacities,[20] respectively. Owing to the similar molecular architectures of HCMPs and NCMPs, this conclusion should be also applicable to the NCMPs if the residual secondary amine moieties are mostly preserved. However, in stark contrast to the HCMP behavior reported before, the FT-IR spectra of **NCMP2** showed negligible changes except

for a weak peak at 1630 cm^{-1} which is slightly increased when oxidized by H_2O_2 or iodine and reduced by anhydrous hydrazine (Figure S15), respectively. This peak may be attributed to the small fraction of quinones existing in the conjugated polymer, which are sensitive to oxidation and reduction. The results indicate that a more stable structure is obtained for NCMPs compared to HCMPs. This is also supported by the negligible changes observed in the ^{13}C NMR spectra of **NCMP2** upon oxidization and reduction (Figure S16). The treated porous polymers showed very small deviations in CO_2 and iodine uptake capacities (Figs. S17 and Table S9). Meanwhile, five-point N_2 adsorption measurements indicated that only a small decrease of surface area observed in **NCMP2** upon oxidization (256 *vs*. 280 m^2/g) is observed. These results prove that the small fraction of residual secondary amines, inevitably left in the polymers due to incomplete polymerization during network formation, are not sufficient to enable a polyaniline-like switching behavior. It can thus be concluded that the majority of secondary amines of the precursors has been converted into tertiary amines after polymerization. This is further confirmed by the finding that no methylene groups are detectable in NCMPs upon further reaction using diiodomethane as a cross-linker (note that such a cross-linking method has been well-developed for the leucoemeraldine base state of polyaniline[30]). Considering the polymers were purified using concentrated acid (35 wt% HCl) and hot water (75 ºC) overnight, the results further indicate their high physicochemical stability.

Furthermore, NCMP networks with abundant tertiary nitrogen moieties possess the potential to coordinate metal ions and act as catalyst support. In an initial, proof-of-concept study, palladium dichloride ($PdCl_2$) was coordinated to **NCMP2** (as **NCMP1** and **NCMP3** have either a lower specific surface area or lower nitrogen content, and were therefore not considered for this initial study). After $PdCl_2$ was introduced, **NCMP2** showed a significant decrease in surface area from 280 to 26 m^2/g due to the weight gained by introducing Pd species and mainly pore blocking or so. Successful coordination was confirmed by ICP-AES, XRD, and XPS analyses as well as SEM and TEM observations. ICP-AES results showed that 11.8 wt% Pd (theoretical content: 21.3 wt%) and no Fe were present in the network structure. The XRD pattern of **NCMP2-$PdCl_2$** shows four additional crystal reflections at 2θ = 39.9, 46.5, 68.2, and 82.0º (Figure 4a) owing to palladium particles,[67] indicating that the $PdCl_2$ introduced was partially reduced to Pd(0). It has been reported

that electron-rich conjugated polymers with high N-content are able to reduce noble metal ions into metallic particles,[68] which seem to be the case also here. The XPS spectra confirm that C, N, Cl, Pd, and O are present in the **NCMP2-PdCl$_2$** (Figure 4b). The O peak is possibly indicative of readily adsorbed oxygen or water, which is normally found in porous materials.[69] The Pd3d core-level XPS spectrum in Figure 5b shows two broad peaks at 337.2 and 342.4 eV, suggesting the existence of both Pd(0) and Pd(II) in the catalyst.[70,71] The result is consistent with that of recently reported Pd, N, P, and O-doped porous polymer catalysts.[71] The N1s core-level XPS spectrum of pristine **NCMP2** shows one binding energy at 399.7 eV owing to C-N bond of the NPh_3 moiety (Figure 5c). After $PdCl_2$ loading, it becomes less intense and a new signal at a binding energy of 400.1 eV appears (Figure 5d). This signal can be attributed to the $PdCl_2$-coordinated NPh_3 moiety. SEM and TEM images indicate that the catalyst maintain the morphology of sphere-like nanoparticles after $PdCl_2$ impregnation (Figure 2b,e,h and Figure 7a,c), with some dark dots that show the additionally formed Pd nanoparticles.

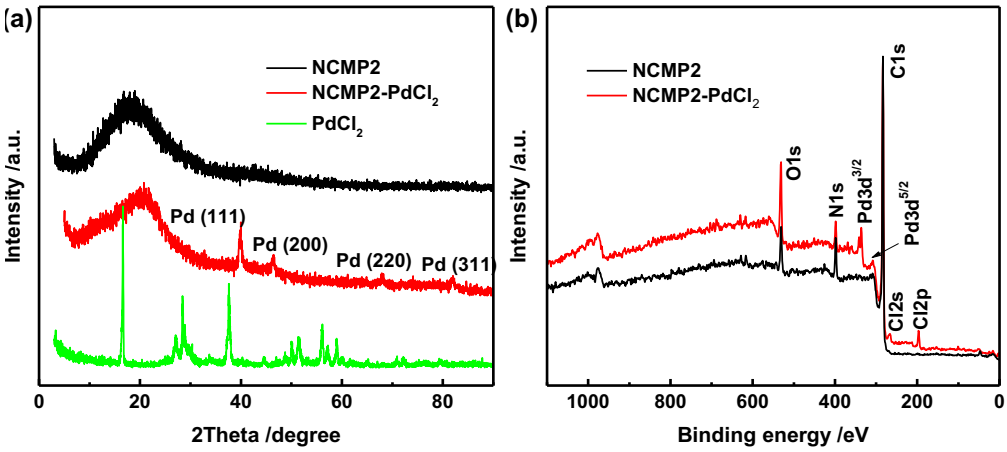

Figure 4 (a) Powder XRD patterns and (b) XPS survey spectra of **NCMP2** and **NCMP2-PdCl$_2$**; $PdCl_2$ is showed for comparison.

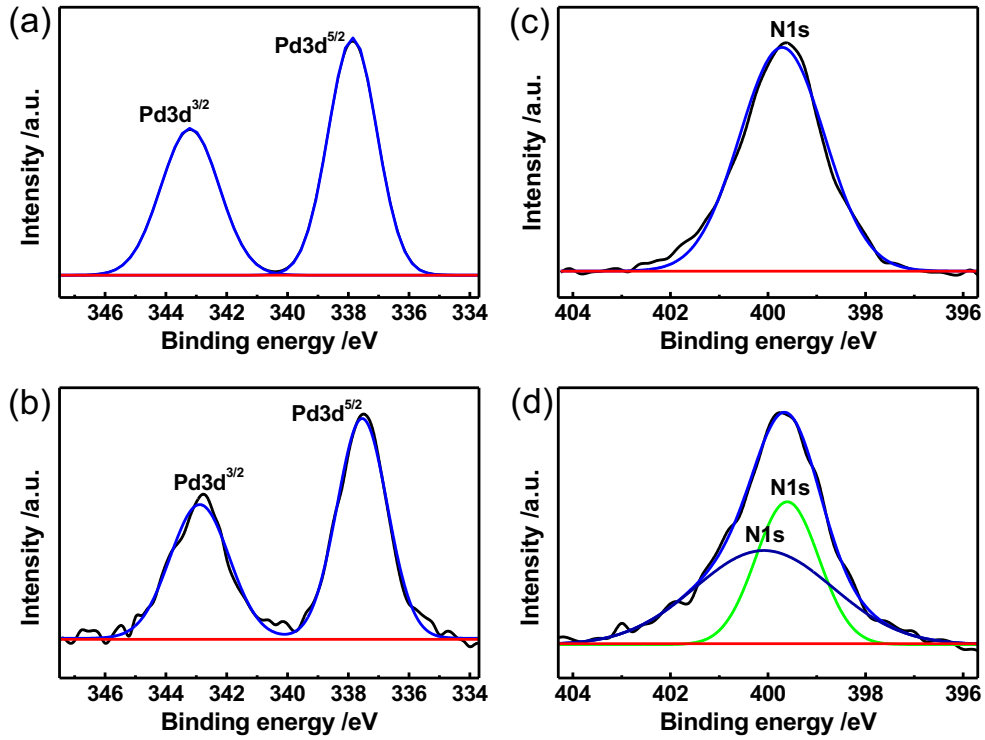

Figure 5 Pd3d (a,b) and N1s (c,d) core-level XPS spectra of (a) **$PdCl_2$**, (c) **NCMP2**, and (b,d) **NCMP2-$PdCl_2$** catalyst.

Applying **NCMP2-$PdCl_2$** as a catalyst enables fast Suzuki–Miyaura coupling reactions in a 60% ethanol aqueous solution under mild conditions (80 ºC). With a series of aryl bromides and benzeneboronic acid used, biaryl products were obtained consistently in high yields (Table 2). The presence of additional Pd(0) nanoparticles within our NMCP materials could play a role and influence the catalytic performance of these materials, and would be valid grounds for further detailed studies into the catalytic behaviour of these complex systems. The **NCMP2-$PdCl_2$** catalyst can be readily recycled by filtration and solvents washes. Applying phenyl bromide and benzeneboronic acid as substrates, the recyclability tests show that the yields of the cross-coupling products remain >94% after six repeat reactions with the recycled catalysts (Figure 6, see supporting information for details of the procedure followed). Control experiments using pristine $PdCl_2$ as catalyst indicated no recyclability (although they showed catalytic activity close to that of the catalyst in presence of **NCMP2** in the first cycle).

Table 2 Suzuki–Miyaura coupling reaction catalyzed by **NCMP2-PdCl$_2$**.

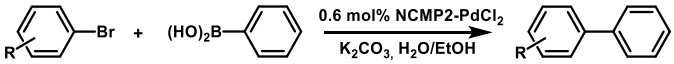

R = H, CH_3, OCH_3, NO_2

Entry	Substrate 1	Substrate 2	Reaction time	Yield
1[a]	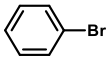	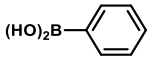	<0.5 h	99.9%
2	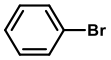	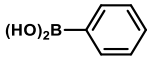	<0.5 h	99.9%
3	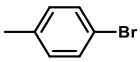	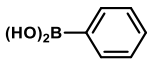	<0.5 h	99.4%
4	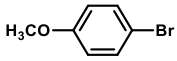	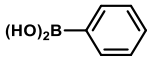	<0.5h	99.9%
5	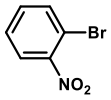	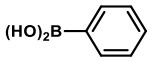	<0.5h	95.1%
6	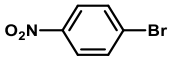	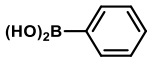	1 h	81.5%
7	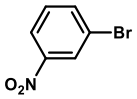	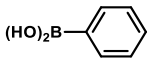	1 h	65.3%

[a] Entry 1: control experiments were done using pristine $PdCl_2$ as the catalyst; Entries 2-7: experiments were done using **NCMP2-PdCl$_2$** as the catalyst.

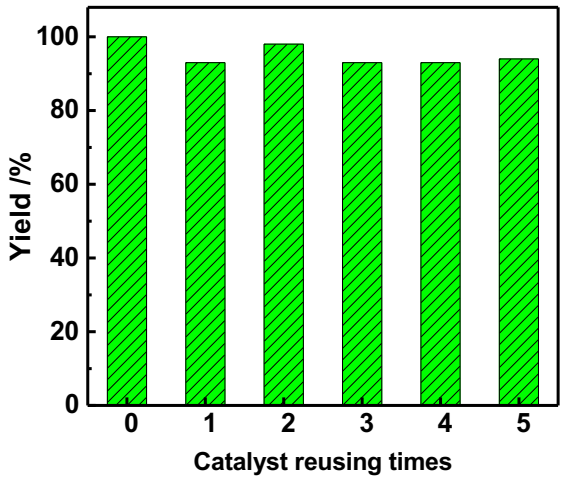

Figure 6 Product yields of Suzuki–Miyaura coupling reaction between phenyl bromide and benzeneboronic acid (Entry 2) using **NCMP2-PdCl$_2$** as a catalyst upon six continuous runs.

The recycled catalyst was also characterized using FT-IR, SEM, TEM, and TGA analyses. The SEM and TEM results showed that the catalyst maintained comparable chemical bonds and morphologies upon using 5 times, suggesting good stability (Figure 7a-d). Note that a strong and broad peak around 3435 cm^{-1} due to water absorption is observed in both catalysts used before and after, as the measurements were carried out in a KBr pellet. TGA scans (under air) showed that the catalyst used before and after maintained a residue of ~10.5 wt% when heated from 540 to 900 ºC, indicating no substantial Pd species leaching occurred from the catalysts during long-term use.

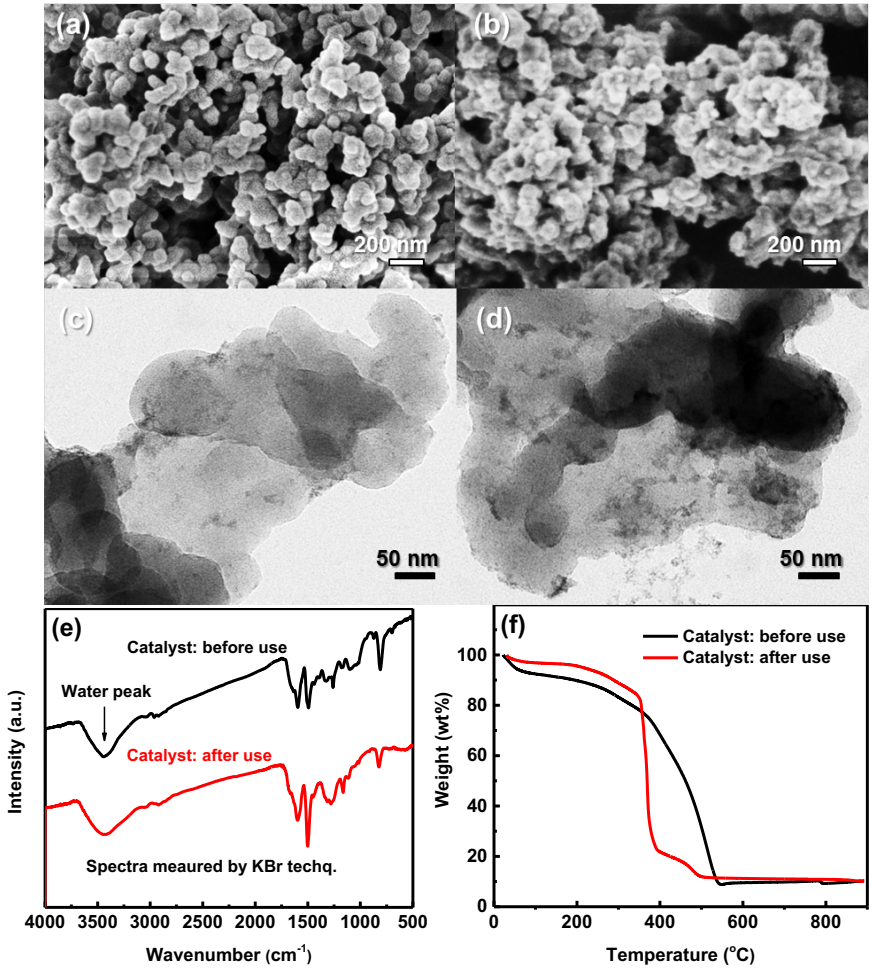

Figure 7 (a,b) SEM and (c,d) TEM images, (e) FT-IR spectra, and (f) TGA scans (under air) of **NMCP2-$PdCl_2$** catalyst before (a,c) and (b,d) after used five times.

The catalytic activity and recyclability of **NCMP2-$PdCl_2$** are competitive with the results recently reported for porous polymers supporting Pd catalysts.[71] Owing to the facile synthesis route, the cheap $FeCl_3$ oxidant involved in polymer synthesis and the high N-content, the here presented

NCMP2 is a convenient and attractive support for metal species.

Conclusions

In summary, three nitrogen-rich conjugated microporous polymers (NCMPs), structurally close to well-known polyaniline, have been prepared at low cost using oxidative coupling of multi-connected aniline precursors. Optimizing molecular architectures of the NCMPs enables moderate CO_2, H_2 and iodine storage abilities as well as good CO_2-selectivity over N_2 at ambient pressure. Owing to their high nitrogen content and porosity, NCMPs can act as a suitable support for $PdCl_2$ coordination and, as a result, such supported catalysts show high activity and recyclability under mild conditions and aqueous reaction media for a model Suzuki–Miyaura coupling reaction. Following on from our investigations and results, we envisage that this functional and versatile family of materials will find future application in catalysis and related uses in the fields of gas and energy storage and conversion.

Acknowledgements

We are grateful to the Alexander von Humboldt Fellowship and Marie Curie Fellowship (YZL, FP7-PEOPLE-2012-IIF TANOGAPPs No. 326385), the National Natural Science Foundation of China (51673039), the Shanghai Pujiang Talent Program (16PJ1400300), and the Fundamental Research Funds for the Central Universities (16D110618) for the generous support of this project. We furthermore acknowledge the support from the Sino-German Center for Research Promotion (GZ879). Initial gas adsorption data were collected on Quantachrome Autosorb-1MP bought under the EPSRC CDT Capital grant (EP/K035746/1).

Supporting information

Experimental details, calculations for atomic electron spin density of the precursors and CO_2/N_2 selectivity, FT-IR, TGA curves, additional CO_2 and H_2 adsorption isotherms, isosteric heat of CO_2 and H_2 adsorption, cyclic voltammetry scans, and summarized chemical/physical properties of NCMPs. Supporting information is available free of charge *via* the Internet at http: //pubs.acs.org.

References

(1) Cooper, A. I. Conjugated Microporous Polymers. *Adv. Mater.* **2009**, *21*, 1291-1295.

(2) Thomas, A. Functional Materials: From Hard to Soft Porous Frameworks. *Angew. Chem. Int.*

Ed. **2010**, *49*, 8328-8344.

(3) Xu, Y. H.; Jin, S. B.; Xu, H.; Nagai, A.; Jiang, D. L. Conjugated Microporous Polymers: Design, Synthesis and Application. *Chem. Soc. Rev.* **2013**, *42*, 8012-8031.

(4) Xie, Y.; Wang, T. T.; Liu, X. H.; Zou, K.; Deng, W. Q. Capture and Conversion of CO_2 at Ambient Conditions by a Conjugated Microporous Polymer. *Nature Commun.* **2013**, *4*, Article number: 1960.

(5) Zhang, Y. G.; Riduan, S. N. Functional Porous Organic Polymers for Heterogeneous Catalysis. *Chem. Soc. Rev.* **2012**, *41*, 2083-2094.

(6) Yuan, K.; Guo-Wang, P. Y.; Hu, T.; Shi, L.; Zeng R.; Forster, M.; Pichler, T.; Chen, Y. W. Scherf, U. Nanofibrous and Graphene-Templated Conjugated Microporous Polymer Materials for Flexible Chemosensors and Supercapacitors. *Chem. Mater.* **2015**, *27*, 7403-7411.

(7) Ding, X. S.; Han, B.-H. Metallophthalocyanine-Based Conjugated Microporous Polymers as Highly Efficient Photosensitizers for Singlet Oxygen Generation. *Angew. Chem. Int. Ed.* **2015**, *54*, 6536-6539.

(8) Liu, X. M.; Xu, Y. H.; Jiang, D. L. Conjugated Microporous Polymers as Molecular Sensing Devices: Microporous Architecture Enables Rapid Response and Enhances Sensitivity in Fluorescence-On and Fluorescence-Off Sensing. *J. Am. Chem. Soc.* **2012**, *134*, 8738-8741.

(9) Chen, L.; Honsho, Y.; Seki, S.; Jiang, D. L. Light-Harvesting Conjugated Microporous Polymers: Rapid and Highly Efficient Flow of Light Energy with a Porous Polyphenylene Framework as Antenna. *J. Am. Chem. Soc.* **2010**, *132*, 6742-6748.

(10) Gu, C.; Huang, N.; Chen, Y. C.; Qin, L. Q.; Xu, H.; Zhang, S. T.; Li, F. H.; Ma, Y. G.; Jiang, D. L. Porous Organic Polymer films with Tunable Work Functions and Selective Hole and Electron Flows for Energy Conversions. *Angew. Chem. Int. Ed.* **2016**, *55*, 3049-3053.

(11) Gu, C.; Chen, Y. C.; Zhang, Z. B.; Xue, S. F.; Sun, S. H.; Zhan, K.; Zhong, C. M.; Zhang, H. H.; Pan, Y. Y.; Lv, Y.; Yang, Y. Q.; Li, F. H.; Zhang, S. B.; Huang, F.; Ma, Y. G. Electrochemical Route to Fabricate Film-like Conjugated Microporous Polymers and Application for Organic Electronics. *Adv. Mater.* **2013**, *25*, 3443-3448.

(12) Kailasam, K.; Mesch, M. B.; Moehmann, L.; Baar, M.; Blechert, S.; Schwarze, M.; Schroeder,

M.; Schomaecker, R.; Senker, J.; Thomas. A. Donor-acceptor-type Heptazine-Based Polymer Networks for Photocatalytic Hydrogen Evolution. *Energy Technol*. **2016**, *4,* 744-750.

(13) Liras, M.; Iglesias, M.; Sánchez, F. Conjugated Microporous Polymers Incorporating BODIPY Moieties as Light-emitting Materials and Recyclable Visible-light Photocatalysts. *Macromolecules* **2016**, *49*, 1666-1673.

(14) Su, C. L.; Tandiana, R.; Tian, B. B.; Sengupta, A.; Tang, W.; Su, J.; Loh, K. P. Visible-light Photocatalysis of Aerobic Oxidation Reactions Using Carbazolic Conjugated Microporous Polymers. *ACS Catal*. **2016**, *6*, 3594-3599.

(15) Liao, Y. Z.; Weber, J.; Faul, C. F. J. Fluorescent Microporous Polyimides Based on Perylene and Triazine for Highly CO_2-selective Carbon Materials. *Macromolecules* **2015**, *48*, 2064-2073.

(16) Germain, J.; Svec, F.; Fréchet, J. M. J. Preparation of Size-selective Nanoporous Polymer Networks of Aromatic Rings: Potential Adsorbents for Hydrogen Storage. *Chem. Mater.* **2008**, *20*, 7069-7076.

(17) Schmidt, J.; Werner, M.; Thomas, A. Conjugated Microporous Polymer Networks via Yamamoto Polymerization. *Macromolecules* **2009**, *42*, 4426-4429.

(18) Bonillo, B.; Sprick, R. S.; Cooper, A. I. Tuning Photophysical Properties in Conjugated Microporous Polymers by Comonomer Doping Strategies. *Chem. Mater.* **2016**, *28*, 3469-3480.

(19) Zhang, P.; Weng, Z. H.; Guo, J.; Wang C. C. Solution-Dispersible, Colloidal, Conjugated Porous Polymer Networks with Entrapped Palladium Nanocrystals for Heterogeneous Catalysis of the Suzuki–Miyaura Coupling Reaction. *Chem. Mater.* **2011**, *23*, 5243-5249.

(20) Liao, Y. Z.; Weber, J.; Mills, B. M.; Ren, Z. H.; Faul, C. F. J. Highly Efficient and Reversible Iodine Capture in Hexaphenylbenzene-Based Conjugated Microporous Polymers. *Macromolecules* **2016**, *49*, 6322-6333.

(21) Liao, Y. Z.; Weber, J.; Faul, C. F. J. Conjugated Microporous Polytriphenylamine Networks. *Chem. Commun*. **2014**, *50*, 8002-8005.

(22) Wang, H. G.; Cheng, Z. H.; Liao Y. Z.; Li, J. H.; Weber, J.; Thomas, A.; Faul, C. F. J. Conjugated Microporous Polycarbazole Networks as Precursors for Nitrogen-enriched

Microporous Carbons for CO_2 Storage and Electrochemical Capacitors. *Chem. Mater.* **2017**, *29*, 4885-4893.

(23) Chen, Q.; Luo, M.; Hammershøj, P.; Zhou, D.; Han, Y.; Laursen, B. W.; Yan, C.-G.; Han, B.-H. Microporous Polycarbazole with High Specific Surface Area for Gas Storage and Separation. *J. Am. Chem. Soc.* **2012**, *134*, 6084-6087

(24) Jiang, F.; Jin, T.; Zhu, X.; Tian, Z. Q.; Do-Thanh, C.-L.; Hu, J.; Jiang, D.-E.; Wang, H. L.; Liu, H. L.; Dai, S. Substitution Effect Guided Synthesis of Task-specific Nanoporous Polycarbazoles with Enhanced Carbon Capture. *Macromolecules* **2016**, *49*, 5325-5330

(25) Sun, C.-J.; Wang, P.-F.; Wang, H.; Han, B.-H. All-Thiophene-Based Conjugated Porous Organic Polymers. *Polym. Chem.* **2016**, *7*, 5031-5038.

(26) Palma-Cando, A.; Brunklaus, G.; Scherf, U. Thiophene-Based Microporous Polymer Networks via Chemical or Electrochemical Oxidative Coupling. *Macromolecules* **2015**, *48*, 6816-6824.

(27) Schmidt, J.; Weber, J.; Epping, J. D.; Antonietti, M.; Thomas, A. Microporous Conjugated Poly(thienylene arylene) Networks. *Adv. Mater.* **2009**, *21*, 702-705.

(28) Yang, M.; Liu, Y. J.; Chen, H. B.; Yang, D. G.; Li, H. M. Porous N-Doped Carbon Prepared from Triazine-Based Polypyrrole Network: a Highly Efficient Metal-free Catalyst for Oxygen Reduction Reaction in Alkaline Electrolytes. *ACS Appl. Mater. Interfaces* **2016**, *8*, 28615-28623.

(29) Yang, M.; Chen, H.; Yang, D.; Gao, Y.; Li, H. Using Nitrogen-Rich Polymeric Network and Iron (II) Acetate as Precursors to Synthesize Highly Efficient Electrocatalyst for Oxygen Reduction reaction in Alkaline Media. *J. Power Sources* **2016**, *307*, 152-159.

(30) Germain, J.; Fréchet, J. M. J.; Svec, F. Hypercrosslinked Polyanilines with Nanoporous Structure and High Surface Area: Potential Adsorbents for Hydrogen Storage. *J. Mater. Chem.* **2007**, *17*, 4989-4997.

(31) Li, D.; Huang, J. X.; Kaner, R. B. Polyaniline Nanofibers: A Unique Polymer Nanostructure for Versatile Applications. *Acc. Chem. Res.* **2009**, *42*, 135-145.

(32) Liao, Y. Z.; Zhang, C.; Zhang, Y.; Strong, V.; Tang, J. S.; Li, X.-G. Kalantar-zadeh, K.; Hoek, E. M. V.; Wang, K. L.; Kaner, R. B. Carbon Nanotube/Polyaniline Composite Nanofibers:

Facile Synthesis and Chemosensors. *Nano Lett*. **2011**, *11*, 954-959.

(33) Liao, Y. Z.; Strong, V.; Chian, W.; Wang, X.; Li, X.-G.; Kaner, R. B. Sulfonated Polyaniline Nanostructures Synthesized via Rapid Initiated Copolymerization with Controllable Morphology, Size, and Electrical Properties. *Macromolecules* **2012**, *45*, 1570-1579.

(34) Pan, L. J.; Yu, G. H.; Zhai, D. Y.; Lee, H. R.; Zhao, W. T.; Liu, N.; Wang, H. L.; Tee, B. C.-K.; Shi,Y.; Cui, Y; Bao, Z. N. Hierarchical Nanostructured Conducting Polymer Hydrogel with High Electrochemical Activity. *Proc. Natl. Acad. Sci. USA* **2012**, *109*, 9287-9292.

(35) Zhai, D. Y.; Liu, B. R.; Shi, Y.; Pan, L. J.; Wang, Y. Q.; Li, W. B.; Zhang, R.; Yu, G. H. Highly Sensitive Glucose Sensor Based on Pt Nanoparticle/Polyaniline Hydrogel Heterostructures. *ACS Nano* **2013**, *7*, 3540-3546.

(36) Aliev, S. B.; Samsonenko, D. G.; Maksimovskiy, E. A.; Fedorovskaya, E. O.; Sapchenko, S. A.; Fedin, V. P. Polyaniline-Intercalated MIL-101: Selective CO_2 Sorption and Supercapacitor Properties. *New J. Chem*. **2016**, *40*, 5306-5312.

(37) Chevalier, J. W.; Bergeron, J. Y.; Dao, L. H. Synthesis, Characterization, and Properties of Poly (*N*-alkylanilines). *Macromolecules* **1992**, *25*, 3325-3331.

(38) Frisch, M. J.; Trucks, G. W.; Schlegel, H. B.; Scuseria, G. E.; Robb, M. A.; Cheeseman, J. R.; Scalmani, G.; Barone, V.; Mennucci, B.; Petersson, G. A.; Nakatsuji, H.; Caricato, M.; Li, X.; Hratchian, H. P.; Izmaylov, A. F.; Bloino, J.; Zheng, G.; Sonnenberg, J. L.; Hada, M.; Ehara, M.; Toyota, K.; Fukuda, R.; Hasegawa, J.; Ishida, M.; Nakajima, T.; Honda, Y.; Kitao, O.; Nakai, H.; Vreven, T.; Montgomery, J. A., Jr.; Peralta, J. E.; Ogliaro, F.; Bearpark, M.; Heyd, J. J.; Brothers, E.; Kudin, K. N.; Staroverov, V. N.; Kobayashi, R.; Normand, J.; Raghavachari, K.; Rendell, A.; Burant, J. C.; Iyengar, S. S.; Tomasi, J.; Cossi, M.; Rega, N.; Millam, J. M.; Klene, M.; Knox, J. E.; Cross, J. B.; Bakken, V.; Adamo, C.; Jaramillo, J.; Gomperts, R.; Stratmann, R. E.; Yazyev, O.; Austin, A. J.; Cammi, R.; Pomelli, C.; Ochterski, J. W.; Martin, E. L.; Morokuma, K.; Zakrzewski, V. G.; Voth, G. A.; Salvador, P.; Dannenberg, J. J.; Dapprich, S.; Daniels, A. D.; Farkas, O.; Foresman, J. B.; Ortiz, J. V.; Cioslowski, J.; Fox, D. J. Gaussian 09 ed.; Gaussian, Inc.: Wallingford CT, **2009**

(39) Cravino, A.; Roquet, S.; Alévêque, O.; Leriche, P.; Frère, P.; Roncali, J. Triphenylamine-Oligothiophene Conjugated Systems as Organic Semiconductors for Opto-electronics. *Chem*.

Mater. **2006**, *18*, 2584-2590.

(40) Chen, Q.; Liu, D.-P.; Luo, M.; Feng, L.-J.; Zhao, Y.-C.; Han, B.-H. Nitrogen-containing Microporous Conjugated Polymers via Carbazole-Based Oxidative Coupling Polymerization: Preparation, Porosity, and Gas Uptake. *Small* **2014**, *10*, 308-315.

(41) Ko, J. H.; Kang, N.; Park, N.; Shin, H.-W.; Kang, S.; Lee, S. M.; Kim, H. J.; Ahn,T. K.; Son, S. U. Hollow Microporous Organic Networks Bearing Triphenylamines and Anthraquinones: Diffusion Pathway Effect in Visible Light-driven Oxidative Coupling of Benzylamines. *ACS Macro Lett*. **2015**, *4*, 669-672.

(42) Zeng, Y. F.; Zou, R. Q.; Zhao, Y. L. Covalent Organic Frameworks for CO_2 Capture. *Adv. Mater.* **2016**, *28*, 2855-2873.

(43) Ren, S. J.; Dawson, R.; Laybourn, A.; Jiang, J. X.; Khimyak, Y.; Adams, D. J.; Cooper, A. I. Functional Conjugated Microporous Polymers: From 1, 3, 5-Benzene to 1, 3, 5-Triazine. *Polym. Chem*. **2012**, *3*, 928-934.

(44) Zhu, X.; Tian, C. C.; Mahurin, S. M.; Chai, S. H.; Wang, C. M.; Brown, S.; Veith,G. M.; Luo, H. M.; Liu, H. L.; Dai, S. A Superacid-Catalyzed Synthesis of Porous Membranes Based on Triazine Frameworks for CO_2 Separation. *J. Am. Chem. Soc*. **2012**, *134*, 10478-10484.

(45) Dawson, R.; Adams, D. J.; Cooper, A. I. Chemical Tuning of CO_2 Sorption in Robust Nanoporous Organic Polymers. *Chem. Sci*. **2011**, *2*, 1173-1177.

(46) Katekomol, P.; Roeser, J.; Bojdys, M.; Weber, J.; Thomas, A. Covalent Triazine Frameworks Prepared From 1,3,5-Tricyanobenzene. *Chem. Mater*. **2013**, *25*, 1542-1548.

(47) Ren, S. J.; Bojdys, M. J.; Dawson, R.; Layboum, A.; Khimyak, Y. Z.; Adams, D. J.; Cooper, A. I. Porous, Fluorescent, Covalent Triazine-based Frameworks via Room-Temperature and Microwave-Assisted Synthesis. *Adv. Mater*. **2012**, *24*, 2357-2361.

(48) Rabbani, M. G.; Islamoglu, T.; El-Kaderi, H. M. Benzothiazole- and Benzoxazole-Linked Porous Polymers for Carbon Dioxide Storage and Separation. *J. Mater. Chem. A* **2017**, *5*, 258-265.

(49) To, J. W. F.; He, J.; Mei, J.; Haghpanah, R.; Chen, Z.; Kurosawa, T.; Chen, S. C.; Bae, W.-G.; Pan, L. J.; Tok, J. B.-H.; Wilcox, J.; Bao, Z. N. Hierarchical N-Doped Carbon as CO_2 Adsorbent with High CO_2 Selectivity From Rationally Designed Polypyrrole Precursor. *J. Am.*

Chem. Soc. **2016**, *138*, 1001-1009.

(50) Chen, C.-X.; Zheng, S.-P.; Wei, Z.-W.; Cao, C.-C.; Wang, H.-P.; Wang, D. W.; Jiang, J.-J.; Fenske, D.; Su, C.-Y. Methane Purification and CO_2/Fluorocarbon Capture. *Chem. Eur. J.* **2017**, *23*, 4060-4064.

(51) Sevilla, M.; Fuerters, A. B. Sustainable Porous Carbons with a Superior Performance for CO_2 Capture. *Energy Environ. Sci.* **2011**, *4*, 1765-1771.

(52) Dawson, R.; Cooper, A. I.; Adams, D. J. Chemical Functionalization Strategies for Carbon Dioxide Capture in Microporous Organic Polymers. *Polym. Int.* **2013**, *62*, 345-352.

(53) Simmons, J. M.; Wu, H.; Zhou, W.; Yildirim, T. Carbon Capture in Metal–Organic Frameworks - A Comparative Study. *Energy Environ. Sci.* **2011**, *4*, 2177-2185.

(54) Sevilla, M.; Fuertes, A. B. Sustainable Porous Carbons with a Superior Performance for CO_2 Capture. *Energy Environ. Sci.* **2011**, *4*, 1765-1771.

(55) Zhu, X.; Do-Thanh, C.-L.; Murdock, C. R.; Nelson, K. M.; Tian, C. C.; Brown, S.; Mahurin, S. M.; Jenkins, D. M.; Hu, J.; Zhao, B.; Liu, H. L.; Dai, S. Efficient CO_2 Capture by a 3D Porous Polymer Derived From Tröger's Base. *ACS Macro Lett.* **2013**, *2*, 660-663.

(56) Germain, J.; Fréchet, J. M. J.; Svec, F. Nanoporous Polymers for Hydrogen Storage, *Small* **2009**, *5*, 1098-1111.

(57) Yang, Y. W.; Tan, B. E.; Wood, C. D. Solution-processable Hypercrosslinked Polymers by Low Cost Strategies: A Promising Platform for Gas Storage and Separation. *J. Mater. Chem. A* **2016**, *4*, 15072-15080.

(58) Yushin, G.; Dash, R.; Jagiello, J.; Fischer, J. E.; Gogotsi, Y. Carbide-Derived Carbons: Effect of Pore Size on Hydrogen Uptake and Heat of Adsorption. *Adv. Funct. Mater.* **2006**, *16*, 2288-2293.

(59) Ben, T.; Ren, H.; Ma, S. Q.; Cao, D. P.; Lan, J. H.; Jing, X. F.; Wang, W. C.; Xu, J.; Deng, F.; Simmons, J. M.; Qiu, S. L.; Zhu, G. S. Targeted Synthesis of a Porous Aromatic Framework with High Stability and Exceptionally High Surface Area. *Angew. Chem. Int. Ed.* **2009**, *121*, 9621-9624.

(60) Wang, Z. G.; Zhang, B. F.; Yu, H.; Sun, L. X.; Jiao, C. L.; Liu, W. S. Microporous Polyimide Networks with Large Surface Areas and Their Hydrogen Storage Properties. *Chem. Commun.*

2010, *46*, 7730-7732.

(61) Furukawa, H.; Yaghi, O. M. Storage of Hydrogen, Methane, and Carbon Dioxide in Highly Porous Covalent Organic Frameworks for Clean Energy Applications. *J. Am. Chem. Soc.* **2009**, *131*, 8875-8883.

(62) Tilford, R. W.; Mugavero III, S. J.; Pellechia, P. J.; Lavigne, J. J. Tailoring Microporosity in Covalent Organic Frameworks. *Adv. Mater.* **2008**, *20*, 2741-2746.

(63) Yu, J. T.; Chen, Z.; Sun, J.; Huang, Z. T.; Zheng, Q. Y. Cyclotricatechylene Based Porous Crystalline Material: Synthesis and Applications in Gas Storage. *J. Mater. Chem.* **2012**, *22*, 5369-5373.

(64) Yang, Z. X.; Xia, Y. D.; Mokaya, R. Enhanced Hydrogen Storage Capacity of High Surface Area Zeolite-like Carbon Materials. *J. Am. Chem. Soc.* **2007**, *129*, 1673-1679.

(65) Ten Hoeve, J. E.; Jacobson, M. Z. Worldwide Health Effects of the Fukushima Daiichi Nuclear Accident. *Energy Environ. Sci.* **2012**, *5*, 8743-8757.

(66) Please note: surface areas, pore sizes and pore size distributions obtained from nitrogen adsorption isotherms at 77 K may be different from the ones at 358 K used for iodine adsorption. Such differences will also contribute to the iodine uptake performance at 358K.

(67) Dhas, N. A.; Gedanken, A. Sonochemical Preparation and Properties of Nanostructured Palladium metallic Clusters. *J. Mater. Chem.* **1998**, *8*, 445-450.

(68) Li, X.-G.; Liu, R.; Huang, M.-R. Facile Synthesis and Highly Reactive Silver Ion Adsorption of Novel Microparticles of Sulfodiphenylamine and Diaminonaphthalene Copolymers. *Chem. Mater.* **2005**, *17*, 5411-5419.

(69) Reiche, S.; Blume, R.; Zhao, X. C.; Su, D.; Kunkes, E.; Behrensa, M.; Schlögl, R. Reactivity of Mesoporous Carbon Against Water – An In-Situ XPS Study. *Carbon* **2014**, *77*, 175-183.

(70) Gao, S. Y.; Huang, Y. B.; Cao, M. N.; Liu, T.-F.; Cao, R. The Fabrication of Palladium-Pyridyl Complex Multilayers and Their Application as a Catalyst for the Heck Reaction. *J. Mater. Chem.* **2011**, *21*, 16467-16472.

(71) Jiang, X. Y.; Zhao, W. X.; Wang, W.; Zhang, F.; Zhuang, X. D.; Han, S.; Feng, X. L. One-Pot Approach to Pd-Loaded Porous Polymers with Properties Tunable by the Oxidation State of

the Phosphorus Core. *Polym. Chem.* **2015**, *6*, 6351-6357.

The table of contents entry

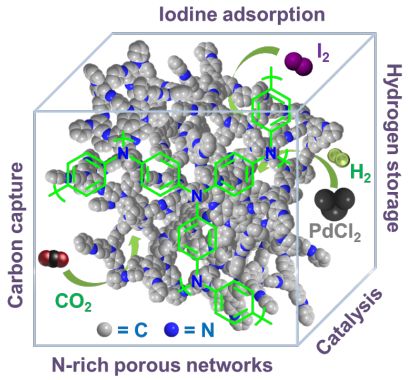

A chemical oxidative polymerization method for facile synthesis of N-rich conjugated microporous polymer networks with high N content and controllable surface area is developed. We demonstrate their use and application as adsorbents for efficient gas storage and recyclable catalyst supports.

Title: Nitrogen-Rich Conjugated Microporous Polymers: Facile Synthesis, Efficient Gas Storage and Heterogeneous Catalysis

Authors: Yaozu Liao, Zhonghua Cheng, Weiwei Zuo, Arne Thomas, Charl F. J. Faul

Keywords: Conjugated microporous polymers, polyaniline, gas storage, catalysis, synthesis